Perturbation theory of quantum solitons: continuum evolution and optimum squeezing by spectral filtering

Dmitry Levandovsky, Michael Vasilyev, and Prem Kumar

Department of Electrical and Computer Engineering, Northwestern University, Evanston, Illinois 60208-3118

Received June 11, 1998

We study the quantum-noise properties of spectrally filtered solitons in optical fibers. Perturbation theory, including a quantum description of the continuum, is used to derive a complete analytical expression for the second-order correlator of the amplitude quadrature. This correlator is subsequently used to optimize the frequency response of the filter numerically in order to achieve the minimum photon-number noise. For propagation distances up to three soliton periods, the length at which the best noise reduction occurs, a square filter is found to be approximately optimum. For longer distances, more-complicated filter shapes are predicted for the best noise reduction. © 1999 Optical Society of America

OCIS codes: 270.6570, 060.5530.

Recently, sub-Poissonian light was generated by frequency filtering of solitons after their propagation through the fiber.[1] Optical solitons were launched into the fiber, and the light emerging from the spectral filter was directed onto a photon-counting detector, where its noise was measured. Numerical and analytical models of these experiments were developed, based on a positive P representation[2] and a backpropagation approach.[3] One critical issue that was not addressed in these models is that of an optimum filter that maximizes the observable quantum-noise reduction for a given length of fiber. In this Letter we offer a solution to the matched-filter problem. We derive, for the first time to our knowledge, an analytical expression for the quantum-noise correlator of the soliton amplitude quadrature as a function of the fiber length, taking into account the complete contribution of the continuum.[4] An experimental study of this correlator was recently reported.[5]

Propagation of the mode-amplitude operator $\hat{a}(\tau, \xi)$ inside an optical fiber is described by the quantum nonlinear Schrödinger equation (NLSE), which in dimensionless coordinates is

$$\frac{\partial}{\partial \xi}\,\hat{a}(\tau,\xi) = i\left[\frac{1}{2}\,\frac{\partial^2}{\partial \tau^2} + \hat{a}^{\dagger}(\tau,\xi)\hat{a}(\tau,\xi)\right]\hat{a}(\tau,\xi)\,. \qquad (1)$$

If the operators in this equation are replaced by c-numbers, Eq. (1) is known to have the classical fundamental-soliton solution $a(\tau, \xi) = \underline{f}_n(\tau)\exp(i\xi/2) \equiv \mathrm{sech}(\tau)\exp(i\xi/2)$, given here in the canonical form corresponding to the average number of photons $\langle \hat{N} \rangle = 2$, where $\hat{N} \equiv \int \hat{a}^{\dagger}(\tau)\hat{a}(\tau)\,\mathrm{d}\tau$. To circumvent the problem of solving for the nonlinear evolution of operator $\hat{a}$, we use the soliton perturbation approach developed in Ref. 6. We write the operator in the following form:

$$\hat{a}(\tau,\xi) = \underline{f}_n(\tau)\exp(i\xi/2) + \Delta\hat{b}(\tau,\xi)$$

$$\equiv [\underline{f}_n(\tau) + \Delta\hat{a}(\tau,\xi)]\exp(i\xi/2)\,, \qquad (2)$$

with $\Delta\hat{a}$ subject to the usual commutation relations everywhere inside the fiber: $[\Delta\hat{a}(\tau, \xi), \Delta\hat{a}(\tau', \xi)] = [\Delta\hat{a}^{\dagger}(\tau, \xi), \Delta\hat{a}^{\dagger}(\tau', \xi)] = 0$, $[\Delta\hat{a}(\tau, \xi), \Delta\hat{a}^{\dagger}(\tau', \xi)] = \delta(\tau - \tau')$. Substituting Eq. (2) into Eq. (1) and keeping only terms that are linear in $\Delta\hat{b}$ divides the analysis of Eq. (1) into two separate problems: the soliton solution of the classical NLSE and the solution of the linearized operator equation

$$\frac{\partial \Delta\hat{b}}{\partial \xi} = \frac{i}{2}\,\frac{\partial^2}{\partial \tau^2}\,\Delta\hat{b} + 2i|a(\tau,\xi)|^2\Delta\hat{b} + ia(\tau,\xi)^2\Delta\hat{b}^{\dagger}, \qquad (3)$$

where the quantum-mechanical fluctuation operator $\Delta\hat{b}$ represents perturbation of the classical soliton field by the quantum noise. This linearization approach is valid if the photon-number noise is small compared with the mean number of photons in the soliton, which is usually the case in most experiments.

In the linearization approximation, because we retain terms only up to first order in $\Delta\hat{b}$, the photon-number noise is determined by the fluctuations in the amplitude quadrature. We assume that the filter $H(\omega)$ at the output of the fiber is linear. Because the filtered light is direct-detected, we can disregard the phase factor $\exp(i\xi/2)$ in Eq. (2), for both the noise and the mean fields, as well as the phase of $H(\omega)$. However, we must restrict the filter transfer function such that $0 \le |H(\omega)| \le 1$ for it to represent a physically realizable filter. In the frequency domain, the fluctuation operator after the filter is

$$\Delta\hat{a}_o(\omega, \xi) = |H(\omega)|\Delta\hat{a}(\omega, \xi) + \sqrt{1 - |H(\omega)|^2}\,\hat{v}(\omega)\,, \qquad (4)$$

where $\hat{v}$ is a vacuum-state operator that describes the frequency-dependent loss of the filter. By normalizing the photon-number variance to the average output photon number we obtain the Fano factor:

$$F(\xi) \equiv \langle \Delta\hat{N}_o(\xi)^2\rangle / \langle \hat{N}_o\rangle = 1 + \langle \hat{N}_o\rangle^{-1} \iint \frac{\mathrm{d}\omega}{2\pi}\,\frac{\mathrm{d}\omega'}{2\pi}$$

$$\underline{f}_n(\omega)\,|H(\omega)|^2 G_N(\omega, \omega', \xi)\,|H(\omega')|^2 \underline{f}_n(\omega')\,, \qquad (5)$$

where $\langle \hat{N}_o\rangle \equiv \int |H(\omega)|^2 \underline{f}_n(\omega)^2 \mathrm{d}\omega/2\pi$ is the average number of photons at the filter output and $G_N(\omega, \omega', \xi)$ is the normally ordered part of the second-order amplitude-quadrature correlator:

0146-9592/99/010043-03$15.00/0

$$G(\omega, \omega', \xi) = 2\pi\delta(\omega - \omega') + G_N(\omega, \omega', \xi)$$
$$\equiv \langle[\Delta\hat{a}(\omega, \xi) + \Delta\hat{a}^\dagger(\omega, \xi)][\Delta\hat{a}(\omega', \xi) + \Delta\hat{a}^\dagger(\omega', \xi)]\rangle .$$

Note that all integrals in Eq. (5) and throughout this Letter are assumed to have limits from $-\infty$ to ∞. Computationally, it is easier to work with a two-dimensional Fourier transform of $G(\omega, \omega', \xi)$:

$$G(\tau, \tau', \xi) = \delta(\tau + \tau') + G_N(\tau, \tau', \xi)$$
$$= \langle[\Delta\hat{a}(\tau, \xi) + \Delta\hat{a}^\dagger(-\tau, \xi)][\Delta\hat{a}(\tau', \xi) + \Delta\hat{a}^\dagger(-\tau', \xi)]\rangle .$$

The solution of Eq. (3) can be written as a normal mode expansion[6]:

$$\Delta\hat{a}(\tau, \xi) = \int \frac{d\Omega}{2\pi}[\hat{V}_c(\Omega, \xi)f_c(\Omega, \tau) + \hat{V}_s(\Omega, \xi)f_s(\Omega, \tau)] + \sum_{i=n,p,\tau,\theta} \hat{V}_i(\xi)f_i(\tau), \quad (6)$$

wherein the four discrete modes f_n, f_p, f_τ, and f_θ represent perturbations to the soliton shape that are due to changes in photon number, momentum (frequency), position (time), and phase, respectively, and f_c and f_s are the symmetric and antisymmetric parts, respectively, of the modes that represent perturbations of the continuum (dispersive radiation) in the fiber. In our convention, the symmetric modes satisfy $f(\tau) = f^*(-\tau)$ and are given by $f_n = [1 - \tau\tanh(\tau)]\mathrm{sech}(\tau)$, $f_p = -i\tau\,\mathrm{sech}(\tau)$, and $f_c = \{[(\Omega^2 - 1) - 2i\Omega\tanh(\tau)]\exp(-i\Omega\tau) + 2\,\mathrm{sech}^2(\tau) \times \cos(\Omega\tau)\}/(\Omega^2 + 1)$, which are real in the frequency domain. The antisymmetric [i.e., $f(\tau) = -f^*(-\tau)$] modes, $f_\tau = \tanh(\tau)\mathrm{sech}(\tau)$, $f_\theta = -i\,\mathrm{sech}(\tau)$, and $f_s = i\{[(\Omega^2 - 1) - 2i\Omega\tanh(\tau)]\exp(-i\Omega\tau) - 2i\,\mathrm{sech}^2(\tau) \times \sin(\Omega\tau)\}/(\Omega^2 + 1)$, are imaginary in ω.

Note that the ξ dependence in Eq. (6) is associated with the operator coefficients $\hat{V}_i$, $\hat{V}_c$, and $\hat{V}_s$ (Heisenberg picture), which are Hermitian. The white coherent-state quantum noise at the input of the fiber ($\xi = 0$) perturbs all the modes of the linearized NLSE, as shown by the expansion in Eq. (6). The operator coefficients in Eq. (6) then propagate through to the end of the fiber, where the noise is reconstructed, once again, by superposition of all the normal modes.

By substituting the expansion in Eq. (6) into Eq. (3) one can show that the photon number and momentum do not change as the soliton propagates along the fiber, i.e., $\hat{V}_n(\xi) = \hat{V}_n(0)$ and $\hat{V}_p(\xi) = \hat{V}_p(0)$, whereas the time and phase evolve according to $\hat{V}_\tau(\xi) = \hat{V}_\tau(0) - \xi\hat{V}_p(0)$ and $\hat{V}_\theta(\xi) = \hat{V}_\theta(0) - \xi\hat{V}_n(0)$. Similarly, for the two continuum operators $\hat{V}_c(\Omega, \xi) = \hat{V}_c(\Omega, 0)\cos[(1 + \Omega^2)\xi/2] + \hat{V}_s(\Omega, 0)\sin[(1 + \Omega^2)\xi/2]$ and $\hat{V}_s(\Omega, \xi) = \hat{V}_s(\Omega, 0)\cos[(1 + \Omega^2)\xi/2] - \hat{V}_c(\Omega, 0)\sin[(1 + \Omega^2)\xi/2]$. Operators $\hat{V}_c$ and $\hat{V}_s$ are essentially the quadrature operators associated with a continuum mode Ω and subject to the usual commutation relations: $[\hat{V}_c(\Omega, \xi), \hat{V}_s(\Omega', \xi)] = i\pi\delta(\Omega - \Omega')$ and $[\hat{V}_c(\Omega, \xi), \hat{V}_c(\Omega', \xi)] = [\hat{V}_s(\Omega, \xi), \hat{V}_s(\Omega', \xi)] = 0$. Note that our continuum mode functions are consistent with the definition in Ref. 6, although we have adopted a form that is convenient for Heisenberg representation.

To project out the expansion coefficients in Eq. (6) one needs to construct an orthogonality relation by pairing the growing solutions with the decaying (adjoint) ones such that the cross energy is conserved.[6] The adjoint solutions, shown here with underbars, are solutions of the adjoint linearized NLSE, which differs from Eq. (3) by the sign of the $\Delta b^\dagger$ term, and are related to the solutions of Eq. (3). Specifically: $\underline{f}_\theta = -if_n$, $\underline{f}_\tau = if_p$, $\underline{f}_s = if_c$, $\underline{f}_n = if_\theta$, $\underline{f}_p = -if_\tau$, $\underline{f}_c = -if_s$ [note that $\underline{f}_n$ is the same as that in Eq. (2)]. Defining the scalar product as

$$\langle f_i \cdot \underline{f}_j^* \rangle = \mathrm{Re}\int f_i(\tau)\underline{f}_j^*(\tau)\mathrm{d}\tau = \mathrm{Re}\int f_i(\omega)\underline{f}_j^*(\omega)\frac{d\omega}{2\pi}, \quad (7)$$

we obtain the orthogonality conditions: $\langle f_i \cdot \underline{f}_j^* \rangle_{i,j\in\{n,p,\tau,\theta,c,s\}} = \Delta_{ij}$, where $\Delta_{ij} = \delta_{ij}$ in all cases except when $i = j \in \{c, s\}$, in which case $\Delta_{ii} = 2\pi\delta(\Omega - \Omega')$.

Only the symmetric (real in the frequency domain) modes contribute to the amplitude-quadrature correlator. Accordingly, we define two time-domain quadrature-like operators, $\Delta\hat{a}_c(\tau, \xi) = [\Delta\hat{a}(\tau, \xi) + \Delta\hat{a}^\dagger(-\tau, \xi)]/2$ and $\Delta\hat{a}_s(\tau, \xi) = [\Delta\hat{a}(\tau, \xi) - \Delta\hat{a}^\dagger(-\tau, \xi)]/2$, where only the symmetric quadrature $\Delta\hat{a}_c(\tau, \xi)$ is needed for our calculation. The quantum-fluctuation operators are projected out by use of Eq. (7), i.e., $\hat{V}_{c,n,p} \equiv \langle\Delta\hat{a}_c \cdot \underline{f}_{c,n,p}^*\rangle$ and $\hat{V}_{s,\theta,\tau} \equiv \langle\Delta\hat{a}_s \cdot \underline{f}_{s,\theta,\tau}^*\rangle$. This projection allows us to obtain an analytical expression for the second-order quadrature correlator in the time domain:

$$G(\tau, \tau', \xi)/4 = \langle\Delta\hat{a}_c(\tau, \xi)\Delta\hat{a}_c(\tau', \xi)\rangle$$
$$= \int \frac{d\Omega}{2\pi}\frac{d\Omega'}{2\pi}\langle\hat{V}_c(\Omega, \xi)\hat{V}_c(\Omega', \xi)\rangle f_c(\Omega, \tau)f_c(\Omega', \tau')$$
$$+ \int \frac{d\Omega}{2\pi}\langle\hat{V}_n\hat{V}_c(\Omega, \xi)\rangle[f_n(\tau)f_c(\Omega, \tau') + f_n(\tau')f_c(\Omega, \tau)]$$
$$+ \int \frac{d\Omega}{2\pi}\langle\hat{V}_p\hat{V}_c(\Omega, \xi)\rangle[f_p(\tau)f_c(\Omega, \tau') + f_p(\tau')f_c(\Omega, \tau)]$$
$$+ \langle\hat{V}_n^2\rangle f_n(\tau)f_n(\tau') + \langle\hat{V}_p^2\rangle f_p(\tau)f_p(\tau'); \quad (8)$$

$$\langle\hat{V}_n\hat{V}_c(\Omega, \xi)\rangle = -(\pi/4)\mathrm{sech}(\pi\Omega/2)\cos[(1 + \Omega^2)\xi/2],$$

$$\langle\hat{V}_p\hat{V}_c(\Omega, \xi)\rangle = (\pi\Omega/12)\mathrm{sech}(\pi\Omega/2)\cos[(1 + \Omega^2)\xi/2],$$

$$\langle\hat{V}_c(\Omega, \xi)\hat{V}_c(\Omega', \xi)\rangle = B(\Omega, \Omega')\cos[(\Omega^2 - \Omega'^2)\xi/2] - A(\Omega, \Omega')\cos[(1 + (\Omega^2 + \Omega'^2)/2)\xi],$$

$$A(\Omega, \Omega') = \frac{(\Omega + \Omega')^2 - 6\Omega\Omega' - 2}{(\Omega^2 + 1)(\Omega'^2 + 1)}\frac{\pi(\Omega + \Omega')/12}{\sinh[\pi(\Omega + \Omega')/2]},$$

$$B(\Omega, \Omega') = \frac{(\Omega - \Omega')^2 + 4}{(\Omega^2 + 1)(\Omega'^2 + 1)}\frac{\pi(\Omega - \Omega')/12}{\sinh[\pi(\Omega - \Omega')/2]} + (\pi/2)\delta(\Omega - \Omega'), \quad (9)$$

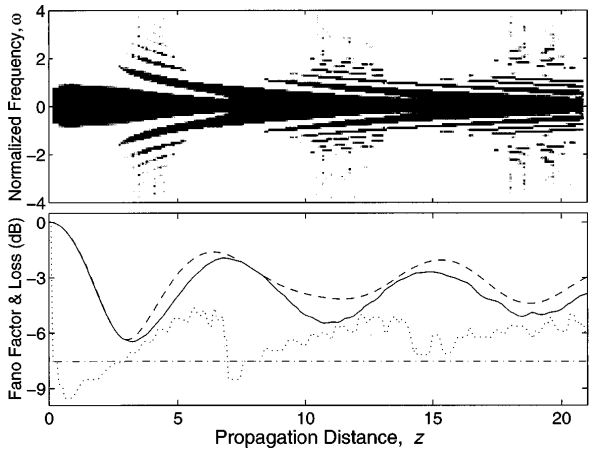

Fig. 1. Top, gray-scale visualization of the optimum filter response $|H(\omega)|^2_{\mathrm{opt}}$, where white and black correspond to 0 and 1, respectively. Bottom, Fano factor obtained for a square filter with $\alpha = 0.18$ (dashed curve) and the optimum filter (solid curve); total loss α for the square filter (dotted–dashed line) and the optimum filter (dotted curve). In both plots distance is in soliton periods.

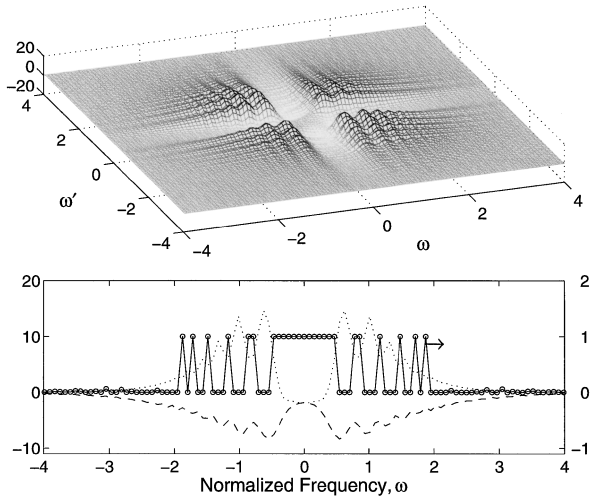

Fig. 2. Top, normally ordered quadrature-noise correlator $G_N(\omega, \omega', \xi)$. Bottom, frequency response $|H(\omega)|^2_{\mathrm{opt}}$ of the optimum filter (interpolated circles), amplitude-quadrature variance $G_N(\omega, \omega, \xi)$ (dotted curve), and zero-frequency-to-sideband correlation function $G_N(0, \omega, \xi)$ (dashed curve). All functions are shown for $z \equiv 2\xi/\pi = 10.73$.

and $\langle \hat{V}_n{}^2 \rangle = 1/2$, $\langle \hat{V}_p{}^2 \rangle = 1/6$.

We have numerically evaluated the integrals in the correlator in Eq. (8) and taken its Fourier transform to get to a form that is useful for the optimum frequency-filtering problem. Note that, in the absence of filtering, only the $\langle \hat{V}_n{}^2 \rangle$ term contributes to the Fano factor, making it equal to 1 because, owing to orthogonality, all the other terms integrate to zero in Eq. (5). This fact makes the role of the filter clear, as it permits mixing in of the negatively correlated terms in Eq. (8). The noise reduction takes place mainly because of the $\langle \hat{V}_n \hat{V}_c \rangle$ term, which describes the fact that an increasing photon number causes an increased soliton bandwidth, thereby resulting in a higher loss introduced by the spectral filter. We observe here that the physical symmetry of the problem suggests an optimum filter function that is even in the frequency domain. Hence the terms that contain f_p do not contribute to the optimally filtered noise.

With the form of the noise correlator in hand, we are able to find the optimum filter frequency response $|H(\omega)|^2_{\mathrm{opt}}$ by minimizing the Fano factor. Because of the constraint that $0 \le |H(\omega)|^2 \le 1$, analytical optimization by variational methods is impractical. Instead, we utilized a numerical quasi-Newton constrained optimization algorithm. The resultant filter shape along with the corresponding Fano factor and the filter loss $\alpha \equiv [1 - \langle \hat{N}_o \rangle / \langle \hat{N} \rangle]$ is shown in Fig. 1 as a function of the propagation distance $z \equiv 2\xi/\pi$ in soliton periods. We have also plotted the results for a square filter with its transmission bandwidth adjusted ($\alpha \approx 0.18$) for maximum noise reduction at $z = 3$. For this filter our results are in an excellent agreement with those in Ref. 3. As can be seen from Fig. 1, the best noise reduction of $\approx$6.5 dB is achieved for $z \approx 3$, where the optimum filter is close to a square shape. The effect of optimization becomes evident for $z > 3$, where the optimum filter acquires more-complicated shapes to take advantage of the fast oscillations that develop in the continuum part of the correlator $G_N(\omega, \omega', \xi)$, as illustrated in Fig. 2.

In conclusion, it is mainly the correlations between the continuum and the soliton photon number that lead to the quantum-noise reduction after spectral filtering. We found the optimum filter that establishes a theoretical limit on the observable noise reduction. For the fiber lengths up to three soliton periods, at which the best noise reduction occurs, the square filter is shown to be a good approximation to the optimum filter. For longer lengths, however, the optimum filter shape develops a number of sidebands, resulting in a clear improvement over the square filter.

The authors acknowledge useful discussions with A. Mecozzi and J. Nocedal. This work was supported in part by the U.S. Office of Naval Research.

References

1. S. R. Friberg, S. Machida, M. J. Werner, A. Levanon, and T. Mukai, Phys. Rev. Lett. **77,** 3775 (1996); S. Spälter, M. Burk, U. Strössner, M. Böhm, A. Sizmann, and G. Leuchs, Europhys. Lett. **38,** 335 (1997); S. Spälter, M. Burk, U. Strössner, A. Sizmann, and G. Leuchs, Opt. Express **2,** 77 (1998).
2. M. J. Werner and S. R. Friberg, Phys. Rev. Lett. **79,** 4143 (1997).
3. A. Mecozzi and P. Kumar, Opt. Lett. **22,** 1232 (1997).
4. D. Levandovsky, M. Vasilyev, and P. Kumar, in *International Quantum Electronics Conference*, Vol. 7 of 1998 OSA Technical Digest Series (Optical Society of America, Washington, D.C., 1998), p. 131.
5. S. Spälter, N. Korolkova, F. König, A. Sizmann, and G. Leuchs, Phys. Rev. Lett. **81,** 786 (1998).
6. D. J. Kaup, Phys. Rev. A **42,** 5689 (1990); H. A. Haus and Y. Lai, J. Opt. Soc. Am. B **7,** 386 (1990); H. A. Haus, W. S. Wong, and F. I. Khatri, J. Opt. Soc. Am. B **14,** 304 (1997).